Dentomaxillofacial Radiology (2013) 42, 20120234

http://dmfr.birjournals.org

RESEARCH

# Radiofrequency heating of metallic dental devices during 3.0 T MRI

M Hasegawa*[,1], K Miyata[1], Y Abe[1] and T Ishigami[1,2]

[1]*Department of Partial Denture Prosthodontics, Nihon University School of Dentistry, Surugadai, Tokyo, Japan;* [2]*Division of Clinical Research, Nihon University School of Dentistry, Surugadai, Tokyo, Japan*

**Objectives:** To estimate the risk of injury from radiofrequency (RF) heating of metallic dental devices in use during 3.0 T MRI.
**Methods:** The whole-body specific absorption rate (WB-SAR) was calculated on the basis of saline temperature elevation under the maximum RF irradiation for 15 min to determine the operation parameters for the heating test. The temperature changes of three types of three-unit bridges, a full-arch fixed dental prosthesis and an orthodontic appliance in use during MRI with a 3.0 T MR system (Magnetom® Verio; Siemens AG, Erlangen, Germany) were then tested in accordance with the American Society for Testing and Materials F2182-09 standardized procedure under the maximum RF heating during 15 min RF irradiation.
**Results:** The system console-predicted WB-SAR was approximately 1.4 W kg$^{-1}$ and that measured with a saline phantom was 2.1 W kg$^{-1}$. In the assessment of RF heating, the highest temperature increase was +1.80 °C in the bridges, +1.59 °C in the full-arch fixed dental prosthesis and +2.61 °C in the orthodontic appliance.
**Conclusions:** The relatively minor RF heating of dental casting material-based prostheses in Magnetom Verio systems in the normal operating mode should not pose a risk to patients. However, orthodontic appliances may exhibit RF heating above the industrial standard (CENELEC standard prEN45502-2-3); therefore, the wire should be removed from the bracket or a spacer should be used between the appliance and the oral mucosa during MRI. *Dentomaxillofacial Radiology* (2013) **42,** 20120234. doi: 10.1259/dmfr.20120234

**Cite this article as:** Hasegawa M, Miyata K, Abe Y, Ishigami T. Radiofrequency heating of metallic dental devices during 3.0 T MRI. *Dentomaxillofac Radiol* 2013; **42:** 20120234.

**Keywords:** magnetic resonance imaging; dental prosthesis; orthodontic appliance; radiofrequency heating

## Introduction

MRI is a useful diagnostic tool for spinal and brain disorders owing to its excellent soft-tissue contrast. Recently, 3.0 T MR scanners have rapidly come to play a significant role in medical diagnostics.[1] MR compatibility is becoming particularly important as the clinical use of high-field scanners (operating mostly at 3 T) is increasing. A primary safety concern related to MRI is metallic medical implant heating by absorbing radiofrequency (RF) energy.[2,3] This risk depends on the metal type, shape and orientation, the static magnetic field strength and the pulse sequence type and parameters.[4–8] American Society for Testing and Materials (ASTM) International, formerly known as the ASTM, requires determination of whether the presence of a passive implant can cause injury to the individual with the implant during MRI. The standard test methods cover measurement of the magnetically induced displacement force on a medical device and RF heating near a passive implant during MRI.[9–12]

Fixed dental prostheses, which are designed depending on the number and location of missing teeth, the method of fabrication and the type of anchorage, are often used to replace or improve the strength and/or aesthetics of teeth. Although recent advances in metal-free materials such as ceramics and composite resins have

*Correspondence to: Mrs M Hasegawa, Department of Partial Denture Prosthodontics, Nihon University School of Dentistry, 1-8-13 Kanda, Surugadai, Chiyoda-Ku, Tokyo 101-8310, Japan. E-mail: hasegawa-mk@dent.nihon-u.ac.jp
Received 28 June 2012; revised 12 October 2012; accepted 24 October 2012

improved the properties of both types of materials,[13–16] metallic prostheses are still commonly used for treatment. Further, orthodontic appliances are used to treat various tooth and jaw irregularities and are important components in fixed orthodontic therapy. During MRI, the temperature rise of metallic implants is greater at areas with large curvature, such as at the tip or loop.[17] Therefore, as with any ferromagnetic device, the presence of an orthodontic appliance or a metallic dental prosthesis in the patient's mouth presents a potentially hazardous situation owing to magnetic field interactions in the MR environment.

In this study, we aimed to estimate the risk of injury from RF heating of metallic dental devices during 3.0 T MRI.

## Materials and methods

We measured the 3.0 T MRI-related RF heating by using a Magnetom® Verio system (syngo MR B17 software; Siemens AG, Erlangen, Germany). This test was conducted in accordance with the ASTM F2182-09 standard test method.[9]

### *Dental devices*

Five metallic dental devices were tested: three bridges, a full-arch fixed prosthesis and an orthodontic appliance. To simulate clinical conditions, maxillary tooth models (D18FE-500A; Nissin Dental Products, Kyoto, Japan) were used for fabricating the devices.

### *Dental prostheses*

For prosthesis fabrication, the thickness of the tooth preparation was 1.7 ± 0.5 mm. Three-unit bridges with the second premolar and second molar as abutments were prepared. The bridges were fabricated with three kinds of dental casting materials (Table 1): silver–palladium–copper–gold alloy (Bridge 1), type III gold alloy (Bridge 2) and alloy for metal–ceramics (Bridge 3). The temperature changes were measured at a mesial point on the second premolar crown, palatal middle point on the first molar crown and distal point on the second molar crown (points 1, 2 and 3, respectively; Figure 1).

A maxillary full-arch fixed prosthesis was also prepared. It comprised 14 abutment crowns cast in silver–palladium–copper–gold alloy; the labial aspect of the anterior teeth had a hard resin facing (Prossimo; GC Co., Tokyo, Japan). The measurement points for this prosthesis were the palatal midline point on the central incisor units (point 4) and distal points on the bilateral second molar units (points 5 and 6; Figure 1).

### *Orthodontic appliance*

The orthodontic appliance comprised an orthodontic bracket and first molar bands attached to a maxillary tooth model (D18FE-500A); orthodontic wire bent in a helical loop at both the mesial and the distal margins of the bilateral canines was attached to the bracket with ligature wires. The temperature was measured after the orthodontic appliance was removed from the tooth model. The measurement points for this device were the palatal midline point on the central incisors (point 7), the labial point on the left canine (point 8) and the distal point on the left second molar (point 9; Figure 1).

### *Saline phantom*

A saline phantom was used to determine the maximum RF irradiation parameters and whole-body specific absorption rate (WB-SAR) before the RF heating test. The phantom consisted of saline solution (2.5 g $l^{-1}$ NaCl dissolved in deionized water) with a conductivity of 0.47 S $m^{-1}$. An acrylic resin container of 65 cm length and 42 cm width was filled with the saline solution to a depth of 9 cm. The saline phantom was insulated with 40 mm thickness of thermal insulation material (Kanelite Super E, Kaneka Corp., Osaka, Japan) on all sides. The conductance of the thermal insulation shell was <0.028 W $mK^{-1}$. The saline phantom was placed in the scanning room for equilibration at least 12 h before the measurements.

### *Determination of RF irradiation parameters and whole-body-averaged SAR*

The WB-SAR was calculated on the basis of saline temperature elevation under the maximum possible RF irradiation for 15 min to ascertain the operation sequence for the RF heating test (Table 2). Temperature

**Table 1** Dental devices evaluated in the radiofrequency heating tests

| *Device* | *Trade name (material)* | *Manufacturer* | *Composition* | *Weight (g)* |
|---|---|---|---|---|
| Bridge 1 | Pallatop 12 Multi (dental silver–palladium–gold alloy) | Dentsply-Sankin, Tokyo, Japan | 12% Au, 20% Pd, 50% Ag and 15% Cu | 9.64 |
| Bridge 2 | K18 (high-gold dental alloy) | GC, Tokyo, Japan | 75% Au, 15% Cu and 9% Ag | 12.83 |
| Bridge 3 | Super Crystal KP-5 (dental casting alloy for porcelain bonding) | Yamamoto Precious Metal, Osaka, Japan | 75% Au, 12% Pd and 7% Pt | 14.80 |
| Full-arch fixed prosthesis | Pallatop 12 Multi (dental silver–palladium–gold alloy) | Dentsply-Sankin, Tokyo, Japan | 12% Au, 20% Pd, 50% Ag and 15% Cu | 24.09 |
| Orthodontic appliance | | | | 2.35 |
| Bracket | KM09012 Integra™ | Rocky Mountain® Orthodontics, Denver, CO | UNS S30400 | |
| Wire | Tru-Chrome® | Rocky Mountain Orthodontics, Denver, CO | UNS S30400 | |
| Band | Truform molar bands | Rocky Mountain Orthodontics, Denver, CO | UNS S30400 | |

UNS, unified numbering system.

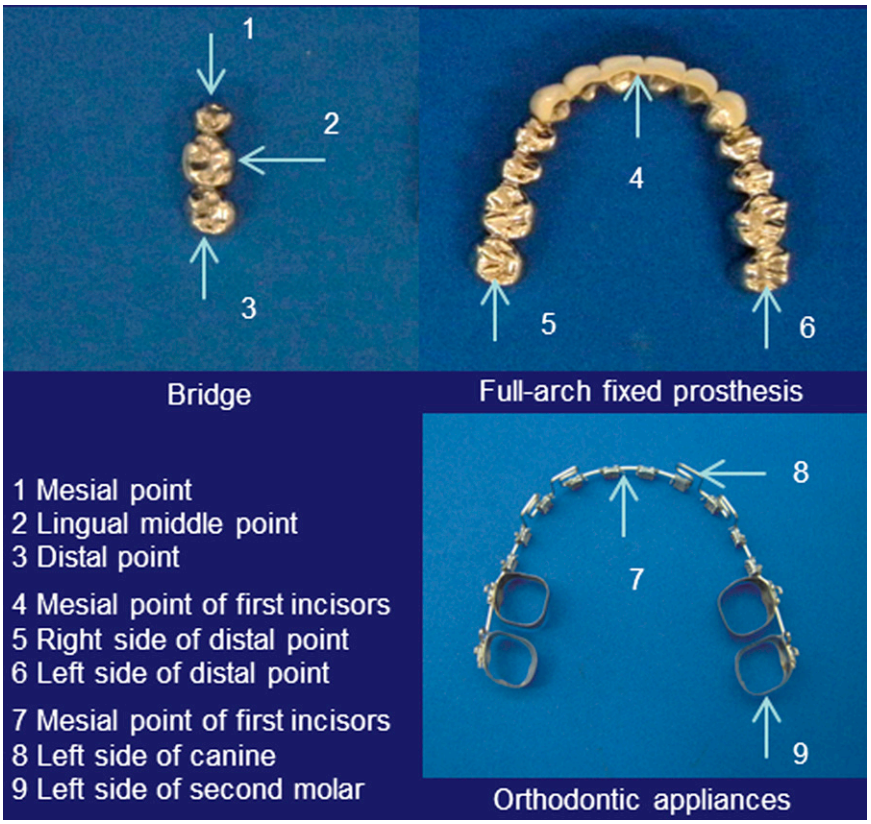


**Figure 1** Dental devices and measurement points

was measured once at each physical location of the saline phantom within the MR scanner and at the centre of the phantom container by using a fibre-optic thermometry system (Luxtron m3300; LumaSense Technologies, Inc., Santa Clara, CA) and fibre-optic thermometry probes (Model MedFP, 0.5 mm in diameter). The probes are unaffected by magnetic forces or RF irradiation and have a resolution of 0.01 °C.

**Table 2** MR sequences for determining the maximum radiofrequency irradiation and whole-body (WB) specific absorption rate (SAR)

| *MR system* | *Magnetom® Verio*[a] |
|---|---|
| Pulse sequence | T-SE |
| Coil | Body coil |
| TR | 864 ms |
| TE | 8.3 ms |
| Echo train length | 5 |
| Plane | Axial |
| Flip angle | 120° |
| Band width | 201 Hz per pixel |
| Field of view | 400 cm |
| Matrix | 256 × 256 |
| Section thickness | 10 mm |
| Total slices | 9 |
| WB-SAR | 1.4 W $kg^{-1}$ |
| NEX | 20 |
| Scan time | 15 min |
| Exposed body SAR | 3.1 W $kg^{-1}$ |
| Head SAR | 0 W $kg^{-1}$ |
| Torso SAR | 7 W $kg^{-1}$ |
| Leg SAR | 7 W $kg^{-1}$ |

NEX, number of excitations; TE, echo time; TR, repetition time; T-SE, turbo spin-echo.
[a]Manufactured by Siemens AG, Erlangen, Germany.

*Tissue-equivalent phantom*

The tissue-equivalent phantom for the RF heating test was prepared with 1.31 g $l^{-1}$ NaCl and 10 g $l^{-1}$ polyacrylic acid in 25 l distilled water. An acrylic resin container of 65 cm length and 42 cm width was filled with the prepared semi-solid gel to a depth of 9 cm (Figure 2). Each dental device was oriented along the longest linear dimension of the phantom, and the phantom was aligned to the magnetic field. The full-arch fixed prosthesis and orthodontic appliance were positioned with their occlusal surfaces directed towards the phantom surface.

*Temperature measurement*

The maximum RF heating during 15 min RF irradiation was achieved on the basis of the predetermined irradiation parameters (Table 2). Fibre-optic thermometers were used to measure the temperature elevations of the dental devices.

The tissue-equivalent phantom was centred in the bore, and the lateral surface of each device was placed 2 cm from its right wall and 2 cm from its surface. The devices and sensors were positioned with implant holders composed of acrylic resin. Temperature was measured by placing the sensors in close contact with the devices, and the difference in temperature before and after RF

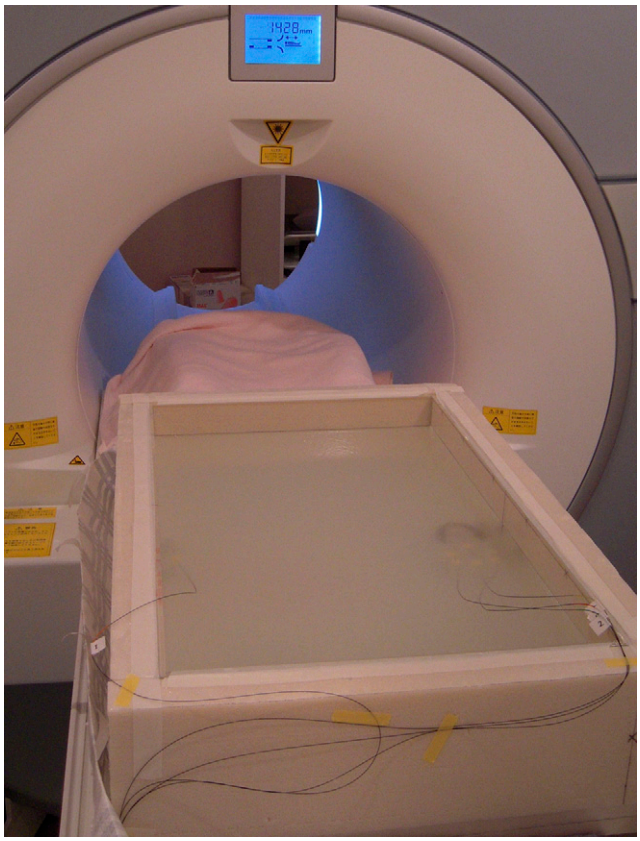

**Figure 2** Tissue-equivalent phantom

irradiation was recorded as the temperature increases. The measurements were performed twice at the same locations, first with the dental devices and then without them (in the gel), to assess the temperature elevation of the devices themselves.

Temperature was recorded at intervals of 1 s from 2 min before to 2 min after RF irradiation. The room temperature was preset to 23 °C, and the tissue-equivalent phantom was placed in the scanning room for equilibration at least 12 h before the measurements.

## Results

The system console-predicted WB-SAR was approximately 1.4 W $kg^{-1}$ and that calculated with the saline phantom was 2.1 W $kg^{-1}$.

The temperature at all the measurement points increased gradually during the irradiation. The temperature elevation of the dental devices at each measurement point is shown in Table 3. Almost all the points showed larger temperature elevations with the dental devices than without them.

The highest temperature increase shown by the bridges was as follows: Bridge 1, approximately +1.80 °C at point 1, which was 1.65 times greater than that at the same point in the gel; Bridge 2, +1.45 °C at point 1, which was 1.33 times greater than that in the gel; and Bridge 3, +1.48 °C at point 3, which was 1.26 times greater than that in the gel. In the full-arch fixed prosthesis, the highest temperature increase was approximately +1.59 °C at point 6, which was 1.67 times greater than that in the gel. In the orthodontic appliance, the highest temperature increase was approximately +2.61 °C at point 9, which was 2.75 times greater than that at the same point in the gel. Overall, the points at the ends of the longest linear dimension of the devices showed the highest temperature elevation.

**Table 3** Temperature elevation of the dental devices at each measurement point

| *Device* | *Maximum temperature increase (°C)* | | |
|---|---|---|---|
| | *Point 1* | *Point 2* | *Point 3* |
| Without bridge | 1.09 | 1.07 | 1.17 |
| Bridge 1 | 1.80 | 1.51 | 1.60 |
| Bridge 2 | 1.45 | 1.21 | 1.39 |
| Bridge 3 | 1.32 | 1.23 | 1.48 |

| | *Point 4* | *Point 5* | *Point 6* |
|---|---|---|---|
| Without full-arch fixed prosthesis | 1.00 | 1.08 | 0.95 |
| Full-arch fixed prosthesis | 1.28 | 0.91 | 1.59 |

| | *Point 7* | *Point 8* | *Point 9* |
|---|---|---|---|
| Without orthodontic appliance | 1.00 | 1.00 | 0.95 |
| Orthodontic appliance | 1.98 | 1.56 | 2.61 |

## Discussion

The growing popularity of MRI suggests that more patients with metallic dental devices will undergo MRI scans. The major concern in this regard is the health risk posed by RF heating of such devices.[2–8] In this study, we estimated this potential hazard to determine the MR compatibility of dental prostheses and orthodontic appliances according to the relevant ASTM standard.[9]

The WB-SAR has been routinely used for reporting the safety of clinical MRI procedures in the presence of conductive implants.[2–9,17,18] However, Baker et al[19] reported that the recorded heating values do not correlate with the console-predicted values of the WB-SAR within a given MR system. Moreover, the methods for WB-SAR calculation by MR systems vary among manufacturers.[19–21] We also reported that the heating of dental magnetic attachments (keeper with coping and implant) is not proportional to the calculated WB-SAR in different-generation 3.0 T MR systems.[18] Therefore, relying on the WB-SAR indicated by an MR system console for establishing implant-related safety may be dangerous. Accordingly, the ASTM F2182-09 standard includes a method of determining the WB-SAR by temperature measurement of an adequate volume of saline.[9]

Saline-based measurement of the WB-SAR is important because the value, which indicates the MR conditional level and is comparable among MR systems, must guarantee that a metallic device does not produce dangerously

high heating in the patient. In this study, the WB-SAR measured with the saline phantom in the Magnetom Verio system under the maximum RF irradiation for 15 min was approximately 2.1 W $kg^{-1}$. However, the system console-predicted value was 1.4 W $kg^{-1}$. Therefore, the predicted and measured WB-SAR values were different.

Most clinical MRI examinations require approximately 30–60 min of total scan time depending on the body part being imaged, ability of the hospital and the patient. However, the ASTM F2182-09 standard test method requires only 15 min of RF irradiation because it is considered to be the reasonable maximum time for a single clinical scan and the temperature tends to increase almost proportionally to the RF irradiation time.[9]

RF heating of dental prostheses can cause great pulpal damage because of the thin layer of residual dentine after tooth preparation.[22,23] In addition, it can damage the cementum, periodontal ligament fibres and alveolar bone because of the proximity of the prosthesis margin to these tissues.[24–26] In the Ottl and Lauer[22] study, 15% of the dental pulps became necrotic when the temperature in the pulp chamber increased by 5.6 °C and 60% became necrotic when the temperature rose by 11.1 °C. Further, Pohto and Scheinin[27] documented increased capillary permeability, which is the first sign of heat-related pulpal damage, when the temperature increased between 5 °C and 7 °C. According to Eriksson and Albrektsson,[24] exposure to temperatures of 44–47 °C (7–10 °C above body temperature) for 1 min is sufficient to cause alveolar bone necrosis. Ramsköld et al[28] also reported that an increase in temperature could be deleterious to tissues adjacent to the tooth, although elevations of 10 °C for 1 min are still considered safe for periodontal tissue, which is less susceptible to thermal damage than bone tissue because of its higher vascularity.[24–26,28] The temperature increase in the dental devices was far below the safety limit of 5.6 °C for pulpal tissue. Although this CENELEC standard prEN45502-1 covers all medical implants, the temperature increase in the orthodontic appliance was above the industrial standard of maximal temperature increase of 2.0 °C, set to limit tissue damage and patient discomfort.

In the assessment of RF heating of the three-unit bridges, the bridge composed of silver–palladium–copper–gold alloy had the highest temperature elevation (+1.80 °C), whereas that made of alloy for metal–ceramics showed the lowest increase. The degree of heating of the full-arch fixed prosthesis, made of silver–palladium–copper–gold alloy, was about the same as that of the silver–palladium–copper–gold alloy bridge, and differences in the volumes of this material were not found. RF-related power depositions as well as an approximate eddy current distribution inside a phantom filled with a conductive medium have been calculated, and the eddy current distribution has been shown to have a circular characteristic along the outer wall of the body.[29] Based on the hypothesis that not all the full-arch fixed prosthesis covers the distribution of the induced E-field spot of the phantom, the heating should be minor. In this test, the orthodontic appliance showed the highest heating (<2.0 °C). This could be explained by the fact that the appliance consisted of an orthodontic bracket, bands, helical loop-shaped orthodontic wires and ligature wires. These formations, which are made up of the ferromagnetic material, would increase the circuit's inductance, and, therefore, large currents would be induced with greater heating of the orthodontic appliance.

In conclusion, we have demonstrated the feasibility of evaluating RF heating of metallic dental devices during MRI examinations. The WB-SAR was determined by measuring saline temperature elevation. The ASTM F2182-09 standard test method provides comparative values of RF power and time.[9] Therefore, the results of this study are applicable to other scan sequences for estimating RF heating by comparing the SAR. The relatively minor RF heating of dental casting material-based prostheses in Magnetom Verio systems in the normal operating mode should not pose a risk to patients. However, orthodontic appliances exhibit heating above CENELEC standard prEN45502-1; therefore, a spacer might be required between the appliance and the oral mucosa or the wire should be removed from the bracket before MRI.

## Acknowledgments

We thank Medical Scanning at Hamamatsu for co-operating with this investigation. This study was supported by a grant from the Dental Research Center, Nihon University School of Dentistry to MH and KM.

## References

1. Willinek WA, Schild HH. Clinical advantages of 3.0 T MRI over 1.5 T. *Eur J Radiol* 2008; **65**: 2–14.
2. Schaefer DJ. Safety aspects of radiofrequency power deposition in magnetic resonance. *Magn Reson Imaging Clin N Am* 1998; **6**: 775–789.
3. Shellock FG. Radiofrequency energy-induced heating during MR procedures: a review. *J Magn Reson Imaging* 2000; **12**: 30–36.
4. Gegauff AG, Laurell KA, Thavendrarajah A, Rosenstiel SF. A potential MRI hazard: forces on dental magnet keepers. *J Oral Rehabil* 1990; **17**: 403–410.
5. Bartels LW, Smits HF, Bakker CJ, Viergever MA. MR imaging of vascular stents: effects of susceptibility, flow, and radiofrequency eddy currents. *J Vasc Interv Radiol* 2001; **12**: 365–371.
6. Shellock FG. Metallic neurosurgical implants: evaluation of magnetic field interactions, heating, and artifacts at 1.5-Tesla. *J Magn Reson Imaging* 2001; **14**: 295–299.
7. Shellock FG, Cosendai G, Park SM, Nyenhuis JA. Implantable microstimulator: magnetic resonance safety at 1.5 Tesla. *Invest Radiol* 2004; **39**: 591–599.

8. Walsh EG, Brott BC, Johnson VY, Venugopalan R, Anayiotos A. Assessment of passive cardiovascular implant devices for MRI compatibility. *Technol Health Care* 2008; **16**: 233–245.
9. American Society for Testing and Materials (ASTM). *ASTM F2182-09 standard test method for measurement of radio frequency induced heating near passive implants during magnetic resonance imaging*. West Conshohocken, PA: ASTM International; 2010.
10. American Society for Testing and Materials (ASTM). *ASTM F2503-05 standard practice for marking medical devices and other items for safety in the magnetic resonance environment*. West Conshohocken, PA: ASTM International; 2005.
11. American Society for Testing and Materials (ASTM). *ASTM F2052-06 standard test method for measurement of magnetically induced displacement force on medical devices in the magnetic resonance environment*. West Conshohocken, PA: ASTM International; 2006.
12. American Society for Testing and Materials (ASTM). *ASTM F2119-07 standard test method for evaluation of MR image artifacts from passive implants*. West Conshohocken, PA: ASTM International; 2007.
13. Freiberg RS, Ferracane JL. Evaluation of cure, properties and wear resistance of Artglass dental composite. *Am J Dent* 1998; **11**: 214–218.
14. Strub JR, Beschnidt SM. Fracture strength of 5 different all-ceramic crown systems. *Int J Prosthodont* 1998; **11**: 602–609.
15. Tinschert J, Natt G, Mautsch W, Augthun M, Spiekermann H. Fracture resistance of lithium disilicate-, alumina-, and zirconia-based three-unit fixed partial dentures: a laboratory study. *Int J Prosthodont* 2001; **14**: 231–238.
16. Ozcan M, Breuklander MH, Vallittu PK. The effect of box preparation on the strength of glass fiber-reinforced composite inlay-retained fixed partial dentures. *J Prosthet Dent* 2005; **93**: 337–345.
17. Muranaka H, Horiguchi T, Usui S, Ueda Y, Nakamura O, Ikeda F. Dependence of RF heating on SAR and implant position in a 1.5T MR system. *Magn Reson Med Sci* 2007; **6**: 199–209.
18. Miyata K, Hasegawa M, Abe Y, Tabuchi T, Namiki T, Ishigami T. Radiofrequency heating and magnetically induced displacement of dental magnetic attachments during 3.0 T MRI. *Dentomaxillofac Radiol* 2012; **41**: 668–674. doi:10.1259/dmfr/17778370
19. Baker KB, Tkach JA, Nyenhuis JA, Phillips MD, Shellock FG, Gonzalez-Martinez J, et al. Evaluation of specific absorption rate as a dosimeter of MRI-related implant heating. *J Magn Reson Imaging* 2004; **20**: 315–320.
20. Baker KB, Nyenhuis JA, Hrdlicka G, Rezai AR, Tkach JA, Shellock FG. Neurostimulation systems: assessment of magnetic field interactions associated with 1.5- and 3-Tesla MR systems. *J Magn Reson Imaging* 2005; **21**: 72–77.
21. Baker KB, Tkach JA, Phillips MD, Rezai AR. Variability in RF-induced heating of a deep brain stimulation implant across MR systems. *J Magn Reson Imaging* 2006; **24**: 1236–1242.
22. Ottl P, Lauer HC. Temperature response in the pulpal chamber during ultrahigh-speed tooth preparation with diamond burs of different grit. *J Prosthet Dent* 1998; **80**: 12–19.
23. Rizoiu I, Kohanghadosh F, Kimmel AI, Eversole LR. Pulpal thermal responses to an erbium, chromium: YSGG pulsed laser hydrokinetic system. *Oral Surg Oral Med Oral Pathol Oral Radiol Endod* 1998; **86**: 220–223.
24. Eriksson AR, Albrektsson T. Temperature threshold levels for heat-induced bone tissue injury: a vital-microscopic study in the rabbit. *J Prosthet Dent* 1983; **50**: 101–107.
25. Saunders EM. In vivo findings associated with heat generation during thermomechanical compaction of gutta-percha. 2. Histological response to temperature elevation on the external surface of the root. *Int Endod J* 1990; **23**: 268–274.
26. Kreisler M, Al-Haj H, D'Hoedt B. Intrapulpal temperature changes during root surface irradiation with an 809-nm GaAlAs laser. *Oral Surg Oral Med Oral Pathol Oral Radiol Endod* 2002; **93**: 730–735.
27. Pohto M, Scheinin A. Microscopic observations on living dental pulp. II. The effect of thermal irritants on the circulation of the pulp in the lower rat incisor. *Acta Odontol Scand* 1958; **16**: 315–327.
28. Ramsköld LO, Fong CD, Strömberg T. Thermal effects and antibacterial properties of energy levels required to sterilize stained root canals with an Nd:YAG laser. *J Endod* 1997; **23**: 96–100.
29. Nordbeck P, Fidler F, Weiss I, Warmuth M, Friedrich MT, Ehses P, et al. Spatial distribution of RF-induced E-fields and implant heating in MRI. *Magn Reson Med* 2008; **60**: 312–319.